Proceedings of the 2006 American Control Conference
Minneapolis, Minnesota, USA, June 14-16, 2006

Dynamic Model-Based Fault Detection and Diagnosis Residual Considerations for Vapor Compression Systems

Michael C. Keir, Andrew G. Alleyne, *Senior Member, IEEE*
Department of Mechanical and Industrial Engineering
University of Illinois at Urbana-Champaign

Abstract - **This paper presents a first look at the dynamic impact of faults on vapor compression systems. Low-order control-oriented dynamic models of subcritical vapor compression cycles are used to develop sensitivity tools that enhance the residual design procedure of dynamic model-based fault detection and diagnosis algorithms. Also, experimental results are presented that confirm the sensitive outputs usefulness in an FDD algorithm. The enhanced fault information carried in the more sensitive signals of a vapor compression system will allow soft faults to be detected earlier, preventing damage to critical system components.**

I. Introduction

VAPOR compression cycles are commonly used for heating and cooling applications in industrial, residential and commercial settings. As a direct result of their widespread use, the energy efficiency of these cycles has received significant attention from the research community. With advancements in compressor and valve technologies, the inclusion of advanced control strategies in these systems has been proposed as a viable means of improving the efficiency of these systems [1]. Advanced control strategies also enable the systems to concurrently attain multiple objectives [2].

Another potential means for improving the energy efficiency of these systems stems from the inclusion of fault detection and diagnosis (FDD) algorithms into their control framework. FDD algorithms can be used to reduce the cost of system maintenance as well as ensure that the system is operating efficiently [3]. In general, current FDD algorithms for vapor compression cycles fall into two categories, steady-state model-based algorithms and neural network/fuzzy model approaches [4].

Dynamic model-based fault detection and diagnosis algorithms, although not prevalent in vapor compression systems, have some important characteristics which could aid in effective fault detection and isolation in air conditioning and refrigeration systems. In order to implement dynamic model-based FDD algorithms a simple dynamic model of vapor compression systems which retains sufficient accuracy is required [1]. In previous work, lumped parameter moving boundary models have been developed for simple vapor compression system components [1,2,5,6]. Recent work has expanded these models to include more complicated system configurations, with components such as receivers and accumulators included in the system model [1]. Since the modeling framework is readily available, the potential advantages of dynamic model-based FDD algorithms in these systems should be identified.

The information currently available in the literature on the dynamic impact of faults on vapor compression systems is quite limited. This paper presents a first look at basic dynamic changes which result from a fault in these systems, and explores the benefits of dynamic model-based fault detection algorithms in vapor compression systems. Existing theoretical tools are shown to be highly effective in identifying the system outputs that are most sensitive to specific faults. This sensitivity information allows the FDD designer to anticipate appropriate sensor locations to most effectively implement their algorithms. In addition, experimental results are presented that confirm the predicted sensitive outputs, and detail how the sensitive signals could be used to structure the residuals to distinguish between similar faults in the evaporator and the condenser.

The remainder of this paper is organized as follows. Section II provides a discussion of the faults common to vapor compression systems. Section III provides a brief summary of the dynamic vapor compression cycle modeling framework. Section IV presents theoretical analysis methods for determining a residual's sensitivity to various faults. Section V presents experimental results which identify appropriate system outputs to include in residual design. Finally, Section VI concludes by highlighting the benefits of improved fault sensitivity in a vapor compression cycle and emphasizes the appropriate outputs to include in a residual to detect an air flow fault in a specific heat exchanger.

II. Air Conditioning and Refrigeration Faults

A number of surveys have been conducted on failures in refrigeration and air-conditioning equipment. Perhaps the most complete survey was performed by Stouppe and Lau in 1989 [7]. This survey summarizes 15,760 failures which occurred between 1980 and 1987 on various air conditioning

This work was supported in part by the sponsoring companies of the Air-Conditioning and Refrigeration Center at the University of Illinois at Urbana-Champaign.

M. C. Keir is a graduate student at the University of Illinois at Urbana-Champaign, Urbana, IL 61801 USA. (email: mkeir2@uiuc.edu)

A. G. Alleyne is a Professor at University of Illinois at Urbana-Champaign, Urbana, IL 61801 USA (phone: 217-244-9993; fax: 217-244-6534; email: alleyne@uiuc.edu).

and refrigeration systems. Of the failures analyzed, 72% were the result of electrical failures. The majority of these electrical failures occurred in the motor windings of the compressor. In 2002, Comstock and Braun [8] conducted a survey of common faults in chillers. They found that 64% of repair costs for chillers were the result of compressor and electrical failures.

In many cases, the electrical failures that occur in the compressor are the result of the compressor being overworked due to soft faults, listed below, forming in the vapor compression system. Soft faults force the system to work over a higher pressure differential, placing additional strain on the compressor that can reduce the lifetime of the compressor windings and decrease system efficiency. In the case of compressor failure, the system is rendered completely inoperative, and the repair costs are often significant. Fault detection algorithms which can detect these soft faults early in their development would reduce the cost of system maintenance by reducing the number of compressor failures [8].

Typical faults which should be included in any comprehensive FDD algorithm for vapor compression cycles are [9]:

- condenser and evaporator fouling
- reductions in mass flow of the external fluid
- refrigerant leaks
- component failures (hard faults)

In many cases component failures are simple to detect due to their abrupt nature and the extreme changes in system behavior which result from the loss of a critical system component [8]. Therefore, the remainder of the discussion in the paper will focus on the detection of soft faults which are more difficult to detect, and are often the cause of the more catastrophic component failures.

III. Dynamic Modeling Framework

A basic vapor compression cycle is composed of four primary components: evaporator, compressor, condenser, and an expansion device. Additionally, a high-side receiver and/or low side-accumulator is generally added to the system as a means of storing excess refrigerant and ensuring safe operation during a variety of conditions. Beginning at the condenser inlet, the high-pressure two-phase fluid flows through the condenser rejecting heat. From the condenser the refrigerant flows to the receiver where any excess charge is stored. Liquid from the receiver then flows through an expansion valve and transitions from a liquid to a two-phase mixture at a lower pressure. The refrigerant enters the evaporator, where heat is absorbed as the fluid evaporates. Vapor from the evaporator is compressed to a higher pressure and continues cycling through the system.

The four controllable inputs to this system are assumed to be compressor speed, expansion valve opening, and mass flow rates of air across the evaporator and condenser. A brief summary of the model is included here as necessary background. The interested reader is referred to [1] for a more complete description of the model and the associated derivation. In general, the dynamics of the compressor and expansion valve are found to be significantly faster than the dominant heat exchanger dynamics, and are thus modeled with static semi-empirical relationships.

A. Evaporator

Modeling of heat exchangers is complicated by the presence of two-phase fluid flow and complex internal and external geometry. The moving boundary approach is based on the assumption of 1-dimensional fluid flow with effective diameter, flow length, and surface areas. The approach also assumes equal pressure throughout the heat exchanger. The heat exchanger is divided into regions based on the fluid phase, and the effective parameters are lumped in each region. The interface between fluid phase regions is allowed to be a dynamic variable.

The derivation procedure for the evaporator requires the integration of the governing partial differential equations (PDEs) along the length of the heat exchanger to remove spatial dependence. The fluid entering the evaporator is assumed to be two-phase, while the fluid exiting the evaporator is superheated vapor. Thus the evaporator is modeled with two regions as shown in Fig. 1.

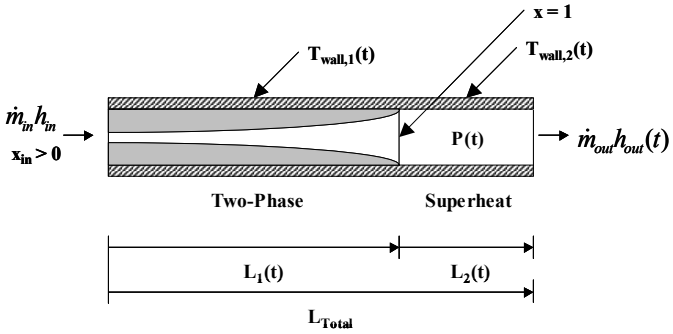

Figure 1 - Evaporator fluid regions and lumped parameters.

The integration of the three conservation equations for each region results in six equations that can be simplified to the nonlinear descriptor form $Z(x,u)\cdot\dot{x} = f(x,u)$, where the elements of $Z(x,u)$ and $f(x,u)$ are nontrivial and presented in detail in [1]. The state variables are defined in terms of pressures, enthalpies, etc. and are the result of the derivation procedure. The states of the evaporator model (x_e) are length of two-phase flow L_{e1}, evaporation pressure P_e, outlet enthalpy $h_{e,out}$, and the two lumped wall temperatures T_{ew1}, and T_{ew2}. The inputs to each of the component models are generally outputs of other component models. The inputs to the evaporator model, u_e, are the inlet and outlet refrigerant mass flow rates $\dot{m}_{e,in}$ and $\dot{m}_{e,out}$ (outputs of the valve and compressor models), the inlet enthalpy $h_{e,in}$ (output of the valve model), and the temperature and mass flow rate of air, $T_{e,air,in}$ and $\dot{m}_{e,air}$ (inputs to the overall system).

$$x_e = \begin{bmatrix} L_{e1} & P_e & h_{e,out} & T_{ew1} & T_{ew2} \end{bmatrix}^T \quad (1)$$

$$u_e = \begin{bmatrix} \dot{m}_{e,in} & \dot{m}_{e,out} & h_{e,in} & T_{e,air,in} & \dot{m}_{e,air} \end{bmatrix}^T \quad (2)$$

B. Condenser with Receiver

The condenser is assumed to have two fluid regions, while a time-varying mean void fraction captures the dynamics associated with small deviations about saturated liquid conditions at the outlet.

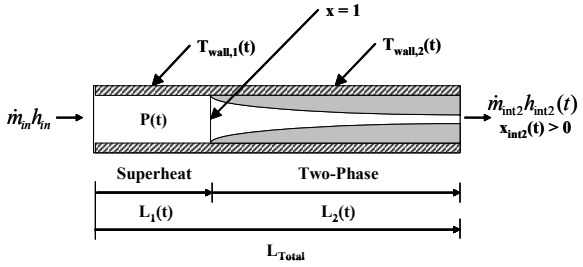

Figure 2 - The fluid region and lumped parameters of the condenser with receiver model.

The governing partial differential equations for mass and energy are integrated along the length of the heat exchanger and lumped parameters are assumed. These six differential equations together with the receiver governing equations are combined to eliminate the intermediate variables, resulting in a model with six states: L_1, P_c, $\bar{\gamma}$, m_{rec}, T_{w1}, and T_{w2}. The resulting model is given in equation (3) and is of the descriptor form $Z(x,u)\cdot\dot{x} = f(x,u)$, where the elements of the Z matrix are nontrivial and given in [1].

$$\begin{bmatrix} z_{11} & z_{12} & 0 & 0 & 0 & 0 \\ z_{21} & z_{22} & z_{23} & z_{24} & 0 & 0 \\ z_{31} & z_{32} & z_{33} & z_{34} & 0 & 0 \\ 0 & z_{42} & 0 & z_{44} & 0 & 0 \\ z_{51} & 0 & 0 & 0 & z_{55} & 0 \\ 0 & 0 & 0 & 0 & 0 & z_{66} \end{bmatrix} \begin{bmatrix} \dot{L}_1 \\ \dot{P} \\ \dot{\bar{\gamma}} \\ \dot{m}_{rec} \\ \dot{T}_{w1} \\ \dot{T}_{w2} \end{bmatrix} = \begin{bmatrix} \dot{m}_i(h_i - h_g) + \alpha_{i1}A_i\left(\frac{L_1}{L_{Total}}\right)(T_{w1} - T_{r1}) \\ \dot{m}_o(h_g - h_{int2}) + \alpha_{i2}A_i\left(\frac{L_2}{L_{Total}}\right)(T_{w2} - T_{r2}) \\ \dot{m}_i - \dot{m}_o \\ \dot{m}_o(h_{int2} - h_f) - UA_{rec}(T_{rec} - T_{amb}) \\ \alpha_{i1}A_i(T_{r1} - T_{w1}) + \alpha_o A_o(T_a - T_{w1}) \\ \alpha_{i2}A_i(T_{r2} - T_{w2}) + \alpha_o A_o(T_a - T_{w2}) \end{bmatrix} \quad (3)$$

C. Compressor and Expansion Valve

The compressor is modeled using volumetric and isentropic efficiencies. A simple first order dynamic is included in the compressor model to account for the thermal capacitance of the compressor shell. The valve expansion process is assumed to be isenthalpic. Both models use empirical maps to account for variations in the operating conditions. A detailed discussion of these models is presented in [1].

D. Linear System Model

For the theoretical analysis presented in this paper the non-linear evaporator and condenser with receiver models were linearized. Connecting the modular components together, an overall system model is generated and can be represented by the standard state space format given in equation (4).

$$\begin{aligned} \dot{\mathbf{x}} &= \mathbf{A}\mathbf{x} + \mathbf{B}\mathbf{u} \\ \mathbf{y} &= \mathbf{C}\mathbf{x} + \mathbf{D}\mathbf{u} \end{aligned} \quad (4)$$

Where **x** is a vector containing the states from both the evaporator and condenser model, and **u** is the vector of external inputs to the system model. The overall system model and the operating conditions around which the system was linearized can be found in [10].

IV. Theoretical FDD Analysis

The ideas of parameter sensitivity are directly applicable to dynamic model-based FDD [10]. Typically it is known how physical parameters are affected by the propagation of a particular fault in a vapor compression system, therefore a model sensitivity analysis that explores perturbations in the parameters can be used to identify the outputs well suited to FDD residual design. Trajectory sensitivity functions are a common method for identifying the dynamic importance of system parameters, as they provide a visual representation of the change in a system's response due to a variation in a particular parameter [11]. Trajectory sensitivity functions, $\delta\mathbf{y}_i$, can be thought of as a first order approximation of the parameter induced error, which is represented by equation (5). $\boldsymbol{\beta}_n$ is the nominal parameter vector, and β_i is the parameter whose sensitivity is being explored. For the following analysis, it is assumed that $\delta\beta_i$ is 10% of the nominal parameter value. The value of 10% is somewhat arbitrary, but it was selected since it represents a fault level that would be desirable to detect, as deviations in parameters larger than 10% may negatively impact the performance of the vapor compression system.

$$\delta\mathbf{y}_i(t,\beta_i) = \left(\frac{\partial\mathbf{y}}{\partial\beta_i}\right)_{\boldsymbol{\beta}=\boldsymbol{\beta}_n}\delta\beta_i \quad (5)$$

The case of external fouling in the evaporator and condenser can be used to examine the effect of parameter variation on system response. The build up of a thermally insulating material on the external surface of a heat exchanger, such as frost on an evaporator or dirt on a condenser, will increase the thermal resistance between the refrigerant and the external fluid. As the layer of material increases in thickness it will impede the flow of the external fluid. The trajectory sensitivity framework can be used to explore the sensitivity of system outputs to changes in a physical parameter that will impact the overall system in a manner similar to the actual fault. In the case of external fouling, the primary effect is a reduction in heat transfer to the external fluid. Therefore, the sensitivity of the vapor compression system model to perturbations in the external heat transfer coefficients for both heat exchangers can be explored, and should provide output sensitivity information relevant to fouling.

To implement the trajectory sensitivity framework, the linear system model from Section III.D can be linearized with respect to a physical parameter. To remove any scaling issues that result from unit discrepancies in the model, both the inputs and outputs were scaled, as shown in equations (6) through (9). The inputs were scaled by their nominal values to provide an equal weighting among the various system inputs. The outputs were scaled to provide the most useful information from an FDD standpoint. Ideally, the analysis should provide the FDD designer with the system outputs that will have the strongest signal to noise ratio. This information can be extracted by scaling the outputs of the trajectory sensitivity analysis by the standard deviation in the measured signal. For example, on our system the

evaporator pressure sensor has a standard deviation of σ_{Pe} = 2.756 kPa according to manufacturer data. The value was verified by running the system at a steady-state operating condition and using an unbiased estimator, resulting in a measured standard deviation of 2.651 kPa. The same verification procedure was used for the condenser pressure sensor, and a value of σ_{Pc} = 8.268 kPa was used in the scaling matrix. There was no manufacturer data on the uncertainty of the thermocouple measurements. Therefore, an unbiased estimator was used and a value of σ_T = 0.12° C was found to represent the uncertainty in the sensors. The scaling will modify analysis to provide the number of standard deviations the faulty output will vary from the normal system output as the result of a 10% change in a particular system input.

$$\begin{bmatrix} \dot{\mathbf{x}} \\ \dot{\boldsymbol{\lambda}} \end{bmatrix} = \begin{bmatrix} \mathbf{A} & \mathbf{0} \\ \dfrac{\partial \mathbf{A}}{\partial \beta_i} & \mathbf{A} \end{bmatrix} \begin{bmatrix} \mathbf{x} \\ \boldsymbol{\lambda} \end{bmatrix} + \begin{bmatrix} \mathbf{B} \\ \dfrac{\partial \mathbf{B}}{\partial \beta_i} \end{bmatrix} \mathbf{W_u u} \tag{6}$$

$$\begin{bmatrix} \mathbf{y} \\ \dfrac{\partial \mathbf{y}}{\partial \beta_i} \end{bmatrix} = \begin{bmatrix} \mathbf{W_y} & \mathbf{0} \\ \mathbf{0} & \mathbf{W_y} \end{bmatrix} \begin{bmatrix} \mathbf{C} & \mathbf{0} \\ \dfrac{\partial \mathbf{C}}{\partial \beta_i} & \mathbf{C} \end{bmatrix} \begin{bmatrix} \mathbf{x} \\ \boldsymbol{\lambda} \end{bmatrix} + \begin{bmatrix} \mathbf{W_y} & \mathbf{0} \\ \mathbf{0} & \mathbf{W_y} \end{bmatrix} \begin{bmatrix} \mathbf{D} \\ \dfrac{\partial \mathbf{D}}{\partial \beta_i} \end{bmatrix} \mathbf{W_u u} \tag{7}$$

$\mathbf{W_u}$ is the weighting matrix given in equation (8), and $\mathbf{W_y}$ is the matrix given in equation (9).

$$\mathbf{W}_u = 0.1 \; diag\left\{ u_v, \; T_{ae,i}, \; \dot{m}_{a,e}, \; \omega_k, \; T_{ac,i}, \; \dot{m}_{a,c} \right\} \tag{8}$$

$$\mathbf{W_y} = diag\left\{ \frac{1}{\sigma_{P_e}}, \frac{1}{\sigma_T}, \frac{1}{\sigma_T}, \frac{1}{\sigma_{P_c}}, \frac{1}{\sigma_T} \right\} \tag{9}$$

Fig. 3 presents the simulated deviation in output response to a 10% step in the valve input command if the evaporator external heat transfer coefficient deviates by 10% from its nominal value. It is clear from the figure that particular system outputs, specifically the evaporator air outlet temperature, are more responsive to the formation of fouling on the external surface of the evaporator. Fig. 4 presents the simulated deviation in output response to a 10% step in the valve input command if the condenser external heat transfer coefficient is reduced by 10% from its nominal value. In this case the most responsive output from a signal to noise perspective is the condenser pressure. Fig. 3 and Fig. 4 indicate the outputs that should be included in a structured or directional residual in an FDD algorithm. For example, if the FDD designer only wished to detect these two fault conditions, the algorithm would require only the measurement of evaporator air outlet temperature and condenser pressure. Although condenser pressure responds to both faults, the evaporator air outlet temperature will only respond to a fault in the evaporator heat transfer coefficient. Hence, the increase in condenser pressure could be used to detect a fault, and the evaporator air outlet temperature signal would indicate the location of the fault.

The reader should also note the difference in scale between the two simulated deviation responses in Fig. 3 and Fig. 4. Clearly, the system outputs explored in this study are more sensitive to changes in the evaporator external heat transfer coefficient. This would imply that a frosted evaporator would be easier to detect than a fouled condenser.

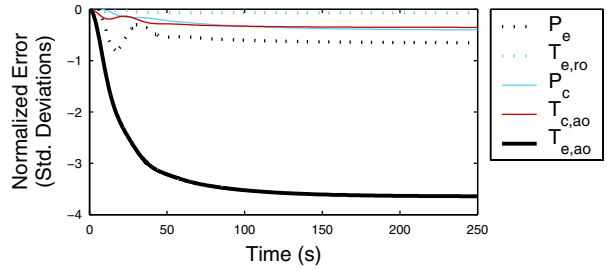

Figure 3 – Change in system response to a valve step as the result of external evaporator fouling.

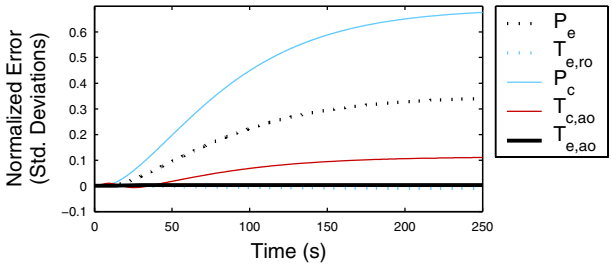

Figure 4 - Change in system response to a valve step as the result of external condenser fouling.

V. Experimental Sensitivity Results

In addition to the theoretical analysis of system changes that result from deviations in physical system parameters, actual faults can be introduced on an experimental test stand to verify the sensitivity of the identified outputs. In general, previous studies have either used a reduction in the mass flow rate of the external fluid or the introduction of a blockage into the external fluid flow path to assess the impact of fouling on a vapor compression system [3,4,9]. In this study, the impact of a reduction in air mass flow rate over each heat exchanger is explored separately.

A. Experimental System

The results presented in this section were taken from an experimental test stand at the University of Illinois at Urbana-Champaign. The test stand has the potential to mimic the behavior of a variety of vapor compression system configurations. The experimental system has a semi-hermetic reciprocating compressor, a single condenser, an array of expansion devices, two evaporators and an internal heat exchanger. The system contains sufficient bypasses and valves to allow the system to be configured in a single or dual evaporator format with the choice of a thermal expansion valve, orifice tube, automatic expansion valve, or an electronic expansion valve regulating the mass flow of the system. The system has five controllable inputs; compressor speed, valve opening, both evaporator fan speeds, and the condenser fan speed. The system is fully instrumented with 6 pressure gauges, 2 mass flow meters, and 24 thermocouples. A complete description of the system can be found in [1].

For the experimental results presented in this paper the system was placed in a single evaporator configuration that bypassed the internal heat exchanger. The electronic expansion valve was used as the expansion device. A block diagram of the configuration used for the experimental results is presented in Fig. 5. A picture of the system is presented in Fig. 6.

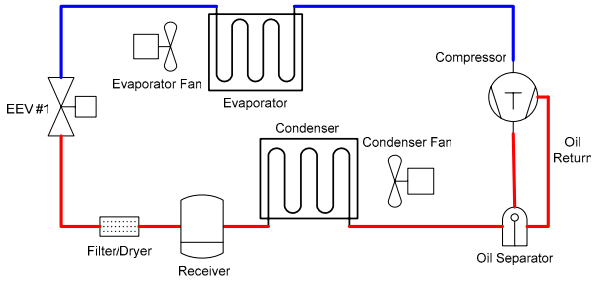

Figure 5 - Diagram of the experimental system configuration.

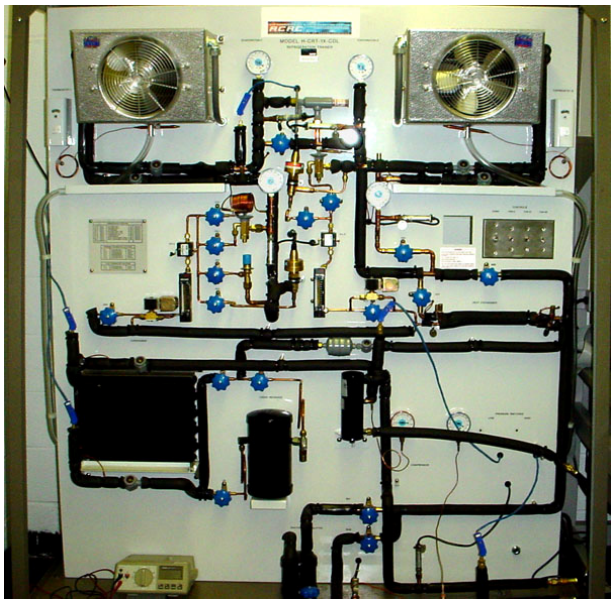

Figure 6 - The experimental test stand located at the University of Illinois at Urbana-Champaign.

B. *Reduction in Evaporator Air Mass Flow Rate*

Consider the impact of a reduction in the air mass flow rate over the evaporator in a vapor compression cycle. This type of fault could be caused by a variety of physical conditions in the system, such as a blockage of the air intake (fouling/frosting), or in a more severe case, a fault in the fan motor. The dynamic and steady state impact of this fault would propagate throughout the system. Therefore, in setting up an FDD algorithm the designer would need to know which system outputs are most sensitive to the fault.

One of the key effects of a reduction in air mass flow rate over a heat exchanger is a decrease in the heat transfer coefficient between the heat exchanger wall and the air. The average air temperature passing over the evaporator coil also decreases, further hindering the heat transfer from the refrigerant to the air. To explore the impact of a reduction in evaporator air mass flow rate, the system was set to run at a steady-state operating condition. With all other inputs held constant, the evaporator air mass flow rate was decreased by 10%. The resulting deviation in output response from the steady-state set point is presented in Fig. 7. In this case, the air mass flow rate decrease occurred at t = 200 seconds, and the outputs were scaled by their sensors standard deviation as in Section IV. This provides the FDD designer with the strongest signals to identify an air mass flow fault in the evaporator. It is clear from the figure that the evaporator air outlet temperature and the evaporator refrigerant outlet temperature respond significantly to an air mass flow fault.

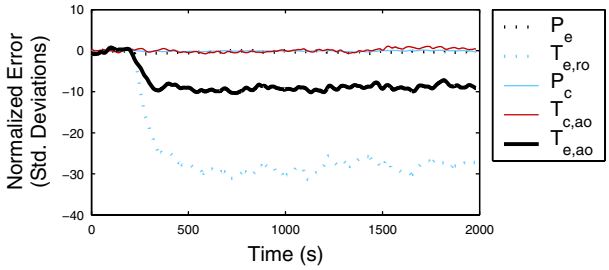

Figure 7 - Output deviation from a 10% decrease in evaporator air mass flow rate.

C. *Reduction in Condenser Air Mass Flow Rate*

In a similar manner to the evaporator air mass flow fault, a 10% fault in the condenser air mass flow rate can be introduced. The level of fault was controlled by reducing the power supplied to the fan, which was correlated to a reduction in the mass flow of air over the heat exchanger. Thus, a specific level of air mass flow fault could be gradually introduced into the condenser. Fig. 8 presents the output deviation resulting from a 10% decrease in condenser air mass flow rate. In general, a vapor compression system is less responsive to a condenser air mass flow fault, therefore the signals were low pass filtered to enhance the visual identification of signal sensitivity. From a visual inspection of Fig. 8, the condenser pressure appears to exhibit a consistent upward drift as a result from the decrease in air mass flow rate. The evaporator air outlet temperature and refrigerant outlet temperature seem to respond in a more oscillatory manner, though this may be partially due to variations in ambient conditions. It should be noted that, as was predicted in Section IV, the size of the deviations as the result of a reduction in condenser air mass flow rate are smaller than those from an equivalent air mass flow rate fault in the evaporator. This would again imply that fouling faults in the evaporator will be easier to detect than a fault of comparable magnitude in the condenser.

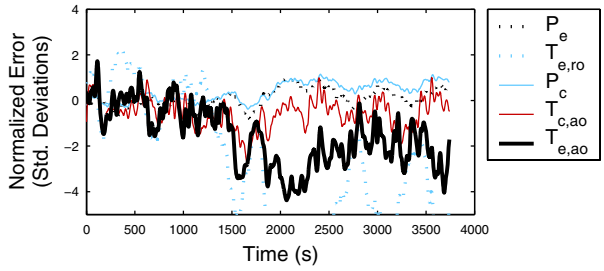

Figure 8 - Output deviation from a 10% decrease in condenser air mass flow rate.

D. FDD Implications

External heat exchanger fouling will impact a vapor compression system in two distinct ways. The build up of a layer of thermally insulating material on the surface of the heat exchanger will increase the thermal resistance between the air and the refrigerant. As the layer increases in size on a conventional tube and fin heat exchanger, the pressure drop across the heat exchanger will increase from the reduction in free flow area through the fins. This will decrease the total mass flow rate of air passing over the heat exchanger. The sensitivity analysis suggested that the condenser pressure and evaporator air outlet temperature would be sufficient to detect the build up of a thermally insulating material on the external surface of the two heat exchangers. From an experimental investigation of the impact of a reduction in air mass flow rate, it was seen that these two outputs do in fact respond significantly to the air flow fault. The sensitivity analysis did not capture all of the signals that would respond, as seen by comparing the refrigerant outlet temperature response in Fig. 3 and Fig. 7. This is likely due to the fact that the sensitivity analysis introduces a change in a single physical parameter to approximate the combined effects parametric and input effects that result from an actual fault.

Although the sensitivity analysis may underestimate the effects of certain input-output variables, it is important to note that it was successful in identifying the following characteristics:

- Condenser fouling is harder to detect than evaporator fouling.
- The evaporator air outlet temperature and condenser pressure can be used to detect and distinguish fouling faults in the evaporator and condenser.

The FDD designer could use the sensitivity information to create a structured or directional residual [12]. With an appropriate residual structure the algorithm will be able to distinguish between different types of faults within the vapor compression system.

VI. Conclusion

Dynamic model-based FDD algorithms offer significant benefits for handling the transient nature under which many vapor compression systems operate. The models allow both steady-state and dynamic parameters to be used in the design of FDD residuals, making the algorithm sensitive to the soft faults which are common to these systems.

Effective FDD algorithms that provide early detection of soft faults in vapor compression systems will result in improved system performance and will significantly reduce the number of catastrophic failures that occur. These combined factors make the inclusion of FDD algorithms in vapor compression systems an integral part of improving the air comfort, refrigeration, and reliability provided by these systems over a wide range of applications. Future research will use the tools presented in this paper to develop and implement a dynamic model-based FDD algorithm on a vapor compression system.

Nomenclature

Variable	Explanation	Subscript	Explanation
T	Temperature	f	Liquid
P	Pressure	g	Vapor
h	Enthalpy	i	Inner
u	Internal Energy	o	Outer
Cp	Specific Heat	T	Total
ρ	Density	ave	Average
α	Heat Transfer Coefficient	cs	Cross-Sectional
$\dot{m}$	Mass Flow Rate	r	Refrigerant
A	Area	w	Wall
L	Length	e	Evaporator
V	Volume	c	Condenser
x	Model States, Quality	v	Valve
u	Model Inputs	int1	Interface 1
β	Model Parameter	n	Nominal

References

[1] B. P. Rasmussen, "Dynamic Modeling and Advanced Control of Air-Conditioning and Refrigeration Systems," Phd. dissertation, Dept. Mech. Eng., University of Illinois at Urbana-Champaign, Urbana, IL, 2005.

[2] X. D. He, S. Liu, and H. Asada, "Modeling of Vapor Compression Cycles for Multivariable Feedback Control of HVAC System," *Journal of Dynamic Systems, Measurement and Control*, vol. 119, no. 2, pp. 183-191, 1997.

[3] J. E. Braun, "Automated Fault Detection and Diagnostics for Vapor Compression Cooling Equipment," *Journal of Solar Engineering*, vol. 125, pp. 266-274, 2003.

[4] A. K. Halm-Owoo, and K. O. Suen, "Applications of fault detection and diagnostic techniques for refrigeration and air conditioning: a review of basic principles," *Proceedings of the Institution of Mechanical Engineers, Part E: Journal of Process Mechanical Engineering*, vol. 216, no. 3, pp. 121-132, 2002.

[5] B. T. Beck, and G. L. Wedekind, "Generalization of the System Mean Void Fraction Model for Transient Two Phase Evaporating Flows," *Journal of Heat Transfer*, vol. 103, no. 1, pp. 81-85, 1981.

[6] E. W. Grald, and J. W. MacArthur, "A Moving Boundary Formulation for Modeling Time-Dependent Two-Phase Flows," *International Journal of Heat and Fluid Flow*, vol. 13, no. 3, pp. 266-272, 1992.

[7] D. E. Stouppe, and T. Y. S. Lau, "Air Conditioning and Refrigeration Equipment Failures," *National Engineer*, vol. 93, no. 9, pp. 14-17, 1989.

[8] M. C. Comstock, J. E. Braun, and E. A. Groll, "A Survey of Common Faults for Chillers," *ASHRAE Transactions*, vol. 108, no. 1, pp. 819-825, 2002.

[9] I. B. D. McIntosh, W. A. Beckman, and J. W. Mitchell, "Fault Detection and Diagnosis in Chillers- Part 1: Model Development and Application," *ASHRAE Transactions*, vol. 106, pp. 268-282, 2000.

[10] M. C. Keir, B. P. Rasmussen, and A. G. Alleyne, "Parametric Sensitivity Analysis and Model Tuning Applied to Vapor Compression Systems," in *Proc. of IMECE*, Orlando, FL, 2005, paper no. 81645.

[11] J. B. Cruz Jr., *Feedback Systems*, McGraw-Hill, New York, 1972.

[12] Gertler, J., *Fault Detection and Diagnosis in Engineering Systems*, Marcel Dekker, Inc., New York, 1998.